

## Dissociation Cross Sections for 0.5- to 1-MeV $\text{HeH}^+$ Ions in $\text{H}_2$ , He, $\text{N}_2$ , and Ne Gases\*

J. Warren Stearns, Klaus H. Berkner, and Robert V. Pyle

*University of California, Lawrence Radiation Laboratory, Berkeley, California 94720*

and

Bruce P. Briegleb and M. Laird Warren

*California State College at Hayward, Hayward, California 94542*

(Received 8 June 1971)

The cross sections for the dissociation modes  ${}^4\text{He}^1\text{H}^+ \rightarrow \text{He}^0 + \text{H}^0$ ,  $\text{He}^0 + \text{H}^+$ ,  $\text{He}^+ + \text{H}^0$ ,  $\text{He}^+ + \text{H}^+$ ,  $\text{He}^{++} + \text{H}^0$ , or  $\text{He}^{++} + \text{H}^+$  are reported for the  $\text{HeH}^+$  energy range of 0.5–1 MeV in the target gases  $\text{H}_2$ , He,  $\text{N}_2$ , and Ne. Comparisons are made with available previous measurements.

### I. INTRODUCTION

The  $\text{HeH}^+$  ion has been the subject of numerous investigations. Calculations of potential-energy curves for electronic states<sup>1</sup> and energy levels of vibrational states have been reported,<sup>2</sup> as well as measurements of cross sections for the formation of the ion,<sup>3</sup> electric field dissociation of the high vibrational states,<sup>2</sup> and the angular distribution of dissociation fragments.<sup>4–6</sup> However, only a few results have been reported for the collisional dissociation cross sections for the  $\text{HeH}^+$  ion: From radial attenuation of the internal beam of a cyclotron, Fremlin and Spiers deduced a destruction cross section in air in the MeV energy range.<sup>7</sup> Wilson has reported destruction cross sections in  $\text{H}_2$ , He, and  $\text{N}_2$  at 50, 100, and 560 keV and cross sections for the formation of  $\text{He}^+$ ,  $\text{He}^0$ , and  $\text{He}^0 + \text{H}^0$  at 560 keV.<sup>2</sup> The only other work on collisional dissociation of which we are aware was by Barnett *et al.*, who did not report cross sections but noted that at 100 keV the principal reaction was electron capture to form the unstable  $\text{HeH}$  molecule.<sup>8</sup>

We have measured the cross sections for the various dissociation modes of 0.5–1-MeV  $\text{HeH}^+$  colliding with  $\text{H}_2$ , He,  $\text{N}_2$ , and Ne:  $\text{HeH}^+ \rightarrow \text{He}^0 + \text{H}^0$ ,  $\text{He}^0 + \text{H}^+$ ,  $\text{He}^+ + \text{H}^0$ ,  $\text{He}^+ + \text{H}^+$ ,  $\text{He}^{++} + \text{H}^0$ , or  $\text{He}^{++} + \text{H}^+$ . The lower-energy limit was determined by the performance of our detector system and the upper limit by our accelerator, a 1-MeV van de Graaff.

### II. EXPERIMENTAL ARRANGEMENT AND PROCEDURE

The  $\text{HeH}^+$  ions were formed in a rf ion source which was operated on a mixture of equal amounts (by pressure) of He and  $\text{H}_2$  gas. The ions were accelerated electrostatically and momentum analyzed magnetically before reaching the experimental assembly shown in Fig. 1. Collimators A and B defined the beam before it entered the differentially pumped 10-cm-long gas cell. The emerging beam and its collision products passed through apertures

C and D into the analysis chamber, where a magnet (11.5-cm diam with 2.5-cm gap) separated the products and directed them to an array of Si surface barrier detectors. The diameter of the  $\text{H}^+$  detector was 2.5 cm; the other detectors were 1 cm in diam. The separation between the  $\text{He}^+$  and  $\text{HeH}^+$  components was so small (approximately 1 mm) that they were both recorded on one detector.

Apertures C and D, which were required to accomplish the differential pumping, were of sufficient diameters to assure that the limiting aperture of the detection system was determined by the detectors. To make sure that all reaction products were detected, the detector size was varied for the more highly scattered hydrogen products. This was done by using the large detector in the  $\text{H}^+$  and  $\text{H}^0$  positions, and by partially masking the large detector. The 1-cm-diam detector was found to be large enough to detect all neutral products, but the 2.5-cm-diam detector was required in the  $\text{H}^+$  position.<sup>9</sup>

The position of the detectors was checked by simultaneously sweeping all beams across their detectors with the analysis magnet. As a check for negatively charged reaction products, the analysis magnet was reversed; no negatively charged particles were observed.

The pulses from each detector were amplified,

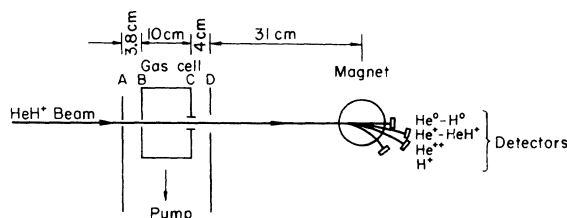


FIG. 1. Experimental arrangement. Beam-defining apertures A and B were 0.127 mm in diam; aperture C was a tube 3.05 mm in diam and 19 mm long; aperture D was 6 mm in diam.

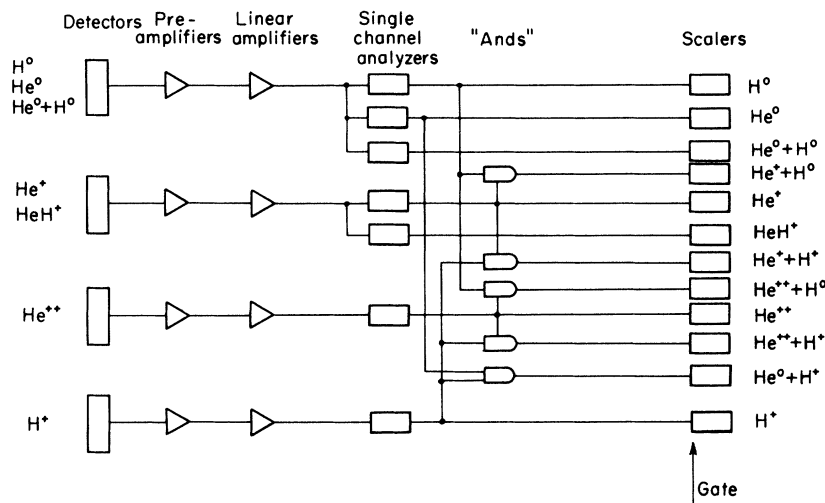


FIG. 2. Counting logic: Gates from the single-channel analyzers drove the scalers and the "and" circuits. Each "and" required simultaneous gates from two sources in order to drive its scaler.

shaped, and sorted by pulse height with single-channel analyzers (Fig. 2). The products from each of the dissociation modes were identified by comparing the corresponding single-channel analyzer outputs in coincidence. Pulses from the single-channel analyzers and the coincidence circuits were recorded with scalers.

The target gas was bled into the target cell through a remotely controlled needle valve and the pressure was monitored with a Datametrix Barocel capacitance manometer. From calibration checks against a McLeod gauge and an oil manometer over a period of several years, we judge the uncertainty in the absolute pressure measurements to be  $\pm 5\%$ . The length of the gas cell was taken to be the distance between collimator B and the midpoint of the tubular exit collimator C.

The background pressure in the approximately 400-cm-long region ahead of collimator A was between  $1 \times 10^{-7}$  and  $1 \times 10^{-6}$  Torr, depending upon the recent history of a Ti sublimation pump located just ahead of the gas cell. The pressure in the analysis region was steady at about  $4 \times 10^{-6}$  Torr and in the differential region it was maintained at less than 1% of the target pressure. All of these pressures were measured with VG1A ion gauges.

The ion energy was determined from the accelerator voltage, which was measured with a generating voltmeter. This was calibrated by observing the  $\gamma$  rays from the nuclear resonance reactions  $^{19}\text{F}(p, \alpha\gamma)^{16}\text{O}$  at 340.5 and 872.5 keV when a Teflon target covered with a grounded tungsten mesh was bombarded with protons.<sup>10</sup> The uncertainty in the ion energy is estimated to be  $\pm 3\%$ .

At each energy the analyzer magnet was set to center the beams on the detectors, and the upper- and lower-level discriminators on the single-channel analyzers were set with the aid of a pulse-height

analyzer. Data were accumulated by counting the pulses from the beam and all its components while the gas cell was maintained at a constant pressure. Measurements were made at 10 to 20 different pressures, from background (approximately  $5 \times 10^{-6}$  Torr) to that which was sufficient to attenuate the incident  $\text{HeH}^+$  beam by 10 to 15% ( $\sim 1$  mTorr in  $\text{N}_2$  and Ne, and  $\sim 3$  mTorr in  $\text{H}_2$  and He).

### III. ANALYSIS

The first step in the data analysis was to determine the total number of incident  $\text{HeH}^+$  ions for each set of data accumulated at a constant pressure. Since we had established that we were detecting all reaction products, the total number of incident  $\text{HeH}^+$  ions could be determined by summing the reaction product pairs and adding this sum to the  $\text{HeH}^+$  counts, which represented the part of the beam that had suffered no collisions. The sum of the reaction products could be determined in three independent ways: by summing  $\text{He}^0 + \text{H}^0$  counts with the coincidence counts, the  $\text{H}^0$  and  $\text{H}^+$  counts, or the  $\text{He}^0$ ,  $\text{He}^+$ , and  $\text{He}^{2+}$  counts. A discrepancy in these three quantities alerted us to a loss of either hydrogen or helium particles or a failure in the coincidence circuits. Once the number of incident ions was determined, the scaler readings could be expressed as fractions of the incident beam.

From the attenuation of the  $\text{HeH}^+$  fraction as a function of target thickness  $\pi$  (the number density of the target gas multiplied by the target length) we obtained the total attenuation cross section  $\sigma_T$ . This was accomplished by a least-squares fit to the expression

$$F_{\text{HeH}^+}(\pi) = F_{\text{HeH}^+}(\pi=0) e^{-\pi\sigma_T}, \quad (1)$$

where  $F_{\text{HeH}^+}(\pi=0)$  is the fraction of the  $\text{HeH}^+$  beam that survives collisions with slits and/or back-

ground gas. This fraction was approximately 0.995.

The change in the fraction of the beam registered in coincidence channel  $i$  is

$$\frac{dF_i}{d\pi} = F_{\text{HeH}^+}(\pi)\sigma_i + \sum_{j \neq i} F_j(\pi)\sigma_{ji} - F_i(\pi) \sum_{j \neq i} \sigma_{ij}, \quad (2)$$

where  $\sigma_i$  is the cross section for the collision that leads to the pair of reaction products  $i$  and  $\sigma_{ji}$  is the cross section for the collision that changes pair  $j$  to pair  $i$ . The partial cross sections  $\sigma_i$  were obtained from a least-squares fit of the data to the second-order solution of Eq. (2). The cross sections  $\sigma_{ij}$ , which were required to correct for secondary collisions, were obtained from Refs. 11-17; in some cases it was necessary to extrapolate to the energies used in this experiment. Precise values for these cross sections were not required, since in the pressure range used in this experiment the inclusion of the second and third terms on the right-hand side of Eq. (2) changes  $\sigma_i$  by less than 10% for most of the cross sections. For the  $\text{He}^{++} - \text{H}^*$  cross section the correction was 15 to 20%.

#### IV. RESULTS AND DISCUSSION

Most of the measurements were made with  $^4\text{He}^1\text{H}^+$  ions. These results are shown in Table I and in Figs. 3-6 for  $\text{H}_2$ , He,  $\text{N}_2$ , and Ne gases. In the table the partial cross sections are labeled by the reaction products of the dissociation mode; e.g., the column headed  $\text{He}^0 + \text{H}^0$  lists the cross section for the dissociation mode  $\text{HeH}^+ \rightarrow \text{He}^0 + \text{H}^0$ . The column labeled  $\sigma_T$  lists the total cross section derived from the measured attenuation of the  $\text{HeH}^+$  beam;  $\Sigma$  is the total-loss cross section obtained by summing the partial cross sections. The two should, of course, be equal, and the close agreement of these two numbers gives an internal consistency

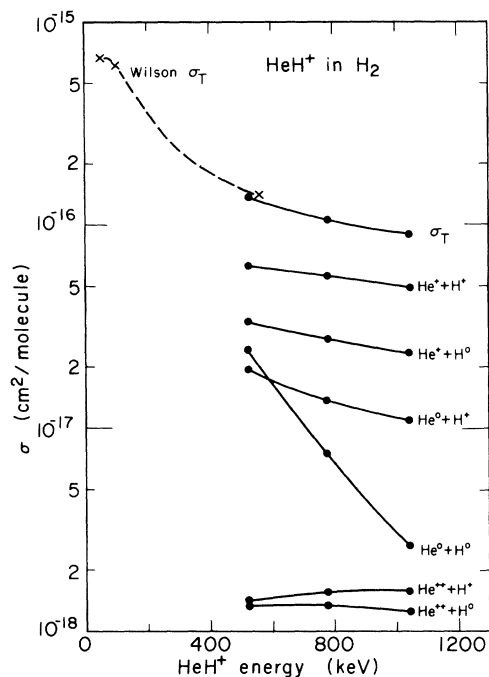


FIG. 3. Dissociation cross sections for  $\text{HeH}^+$  in  $\text{H}_2$ . Cross sections shown are for interactions giving the products indicated at the right of each curve. Lines are shown only to connect the corresponding data points. Data of Wilson for  $\sigma_T$  are indicated by  $x$  and are connected with dashed lines (Ref. 2).

check of our results.

From the reproducibility of the results and the standard deviation of the least-squares fit, we estimate the relative standard error in the cross sections to be  $\pm 5\%$  except as indicated in Table I. In addition there is a possible systematic error, which we estimate as  $\pm 7\%$ , due to uncertainties in the

TABLE I. Cross sections ( $10^{-17} \text{cm}^2/\text{molecule}$ ) for dissociation of  $\text{HeH}^+$ . Relative uncertainties  $\pm 5\%$  except as indicated (systematic uncertainties of  $\pm 7\%$  not included).

Target gas	Energy (keV)	$\sigma_T$	$\sigma$ for indicated products						$\Sigma$
			$\text{He}^0 + \text{H}^0$	$\text{He}^0 + \text{H}^+$	$\text{He}^+ + \text{H}^0$	$\text{He}^+ + \text{H}^+$	$\text{He}^{++} + \text{H}^0$	$\text{He}^{++} + \text{H}^+$	
$\text{H}_2$	525	14.1	2.42	1.91	3.33	6.3	0.134 <sup>a</sup>	0.140 <sup>b</sup>	14.2
	780	10.9	0.75	1.38	2.71	5.6	0.134 <sup>a</sup>	0.158 <sup>a</sup>	10.7
	1045	9.0	0.27 <sup>a</sup>	1.10	2.35	5.0	0.125 <sup>a</sup>	0.160 <sup>c</sup>	9.0
He	505	12.2	3.00	1.25	1.93	5.6	0.164 <sup>a</sup>	0.225 <sup>b</sup>	12.2
	770	9.3	1.16	0.90	1.56	5.3	0.130 <sup>a</sup>	0.225	9.3
	1040	7.5	0.48	0.73	1.30	4.8	0.122 <sup>a</sup>	0.175 <sup>a</sup>	7.6
$\text{N}_2$	525	50.2	5.2	5.9	9.9	24.8	1.81	2.70 <sup>b</sup>	50.3
	780	45.5	2.42	4.0	8.2	24.7	2.09	4.1	45.5
	1045	41.7	1.15	3.45	6.9	24.1	1.84	4.5	41.9
Ne	505	25.4	4.3	2.77	4.4	12.0	0.79	1.37 <sup>b</sup>	25.5
	770	24.0	2.14	2.33	3.77	12.9	0.87	1.98	24.0
	1040	21.7	1.05	1.78	3.22	12.6	0.87	2.15	21.7

<sup>a</sup> $\pm 8\%$ .

<sup>b</sup> $\pm 15-8\%$ .

<sup>c</sup> $\pm 15\%$ .

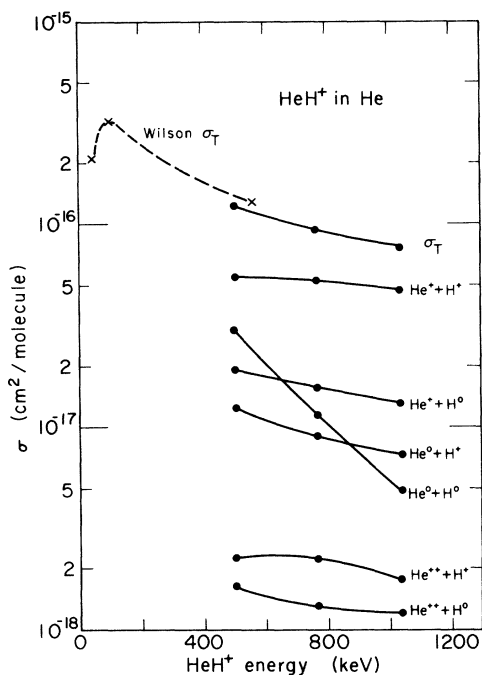


FIG. 4. Dissociation cross sections for  $\text{HeH}^+$  in He. See legend for Fig. 3.

absolute pressure measurements and the effective length of the target. Hence for most of the entries in Table I the absolute uncertainty is about  $\pm 10\%$ .

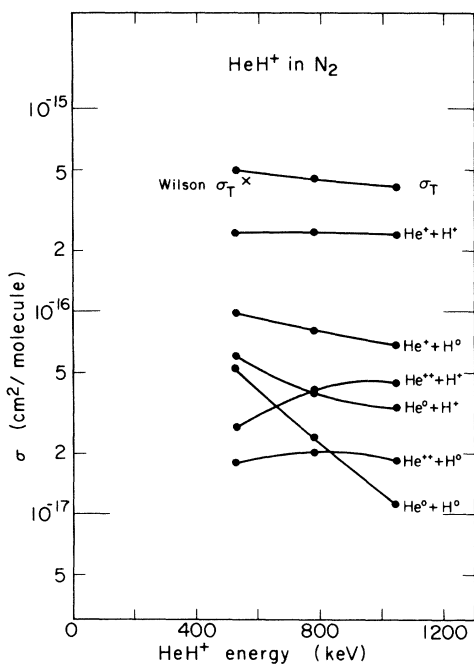


FIG. 5. Dissociation cross sections for  $\text{HeH}^+$  in  $\text{N}_2$ . See legend for Fig. 3.

Also shown in Figs. 3-5 are the total-loss cross sections reported by Wilson.<sup>2</sup> Wilson's partial cross sections for the production of  $\text{He}^*$ ,  $\text{He}^0 + \text{H}^+$ , and  $\text{He}^0 + \text{H}^0$  at 560 keV are compared with our results in Table II. With the exception of the  $\text{He}^0 + \text{H}^0$  cross section, the agreement is good.

The only other  $\text{HeH}^+$  cross section measurement of which we are aware is the total-loss cross section reported by Fremlin and Spiers in the MeV range in air.<sup>7</sup> Their value of  $\sigma E = 1 \times 10^{-14} \text{ cm}^2 \text{ MeV/atom}$  is much larger than our measurement in  $\text{N}_2$ .

To see whether the isotopic composition affected the cross sections, we also measured the dissociation of  $^3\text{HeD}^+$  in  $\text{D}_2$  and  $\text{N}_2$  at 795 keV. For this measurement five detectors were placed at positions appropriate for  $^3\text{He}$  and D fragments. This measurement was complicated by the presence of  $\text{D}_2\text{H}^+$  impurity in the beam which could not be entirely eliminated.<sup>18</sup> A  $\text{D}_2$  target was used because an  $\text{H}_2$  target made the impurity component increase, apparently by migration of minute quantities of  $\text{H}_2$  to the source. The  $\text{D}_2\text{H}^+$  component was approximately 20% of the primary beam; we used the  $\text{H}_3^+$  dissociation results of Ref. 19 to correct for the contribution of this component to our scaler counts. Because of these corrections the uncertainties assigned to the calculated cross sections are about twice those of the  $^4\text{HeH}^+$  values in Table I. Within these uncertainties the cross sections for breakup of  $^4\text{He}^1\text{H}^+$  and  $^3\text{HeD}^+$  ions are the same.

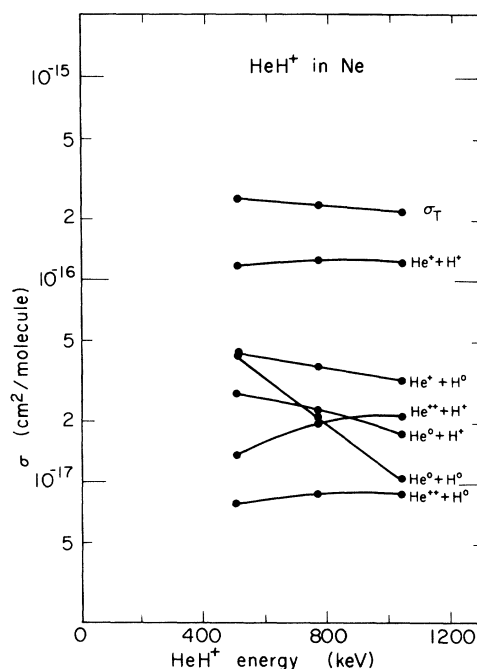


FIG. 6. Dissociation cross sections for  $\text{HeH}^+$  in Ne. See legend for Fig. 3.

TABLE II. A comparison of the results of Wilson (Ref. 2) at 560 keV with the appropriate sum of cross sections from the present work. The values shown, in units of  $10^{-17}$  cm<sup>2</sup>, are from a graphical interpolation of our data. The Wilson results have an uncertainty of  $\pm 20\%$ .

Target Process	H <sub>2</sub>			He			N <sub>2</sub>		
	He <sup>+</sup>	He <sup>0</sup> +H <sup>+</sup>	He <sup>0</sup> +H <sup>0</sup>	He <sup>+</sup>	He <sup>0</sup> +H <sup>+</sup>	He <sup>0</sup> +H <sup>0</sup>	He <sup>+</sup>	He <sup>0</sup> +H <sup>+</sup>	He <sup>0</sup> +H <sup>0</sup>
Wilson	9.1	2.4	3.0	8.3	1.3	3.3	31	5.0	8.8
Present work	9.7	1.8	2.0	7.4	1.2	2.5	35	5.6	4.7

The cross sections reported here represent averages over an unknown population distribution of the vibrational states of the HeH<sup>+</sup> ion.

#### ACKNOWLEDGMENTS

The research on the HeH<sup>+</sup> ion was suggested by Dr. John R. Hiskes in connection with the problem

of fuel injection into controlled thermonuclear fusion mirror devices. V. J. Honey was of great help in the setup and maintenance of the experiment. Two of us (B. P. B. and M. L. W.) would like to thank Associated Western Universities, Inc. for financial support which permitted participation in this experiment.

\*Work performed under the auspices of the U. S. Atomic Energy Commission.

<sup>1</sup>See, for example, the discussion and references in H. H. Michels, *J. Chem. Phys.* **44**, 3834 (1966).

<sup>2</sup>Walter D. Wilson, Lawrence Radiation Laboratory Report No. UCRL-16308, 1965 (unpublished).

<sup>3</sup>See, for example, the discussion and references in the Appendix of Ref. 4.

<sup>4</sup>J. Schopman and J. Los, *Physica* **48**, 170 (1970).

<sup>5</sup>J. Schopman, J. Los, and J. Maas, *Physica* **51**, 113 (1971).

<sup>6</sup>J. Schopman and J. Los, *Physica* **51**, 132 (1971).

<sup>7</sup>J. H. Fremlin and V. M. Spiers, *Proc. Phys. Soc. (London)* **A68**, 398 (1955).

<sup>8</sup>C. F. Barnett, J. A. Ray, and R. M. Warner, Oak Ridge National Laboratory Report No. ORNL-3472, 1963, p. 60 (unpublished).

<sup>9</sup>When the large detector was covered with a mask which reduced its area by 25%, the only observable effect was a 10% reduction in the H<sup>+</sup> counts that were in coincidence with He<sup>++</sup>. Since the counts did not quite reach a plateau at our largest available detector area equivalent to an acceptance angle of  $\pm 25$  mrad measured from the entrance of the gas cell, there is the possibility that we may have missed some of the H<sup>+</sup> from this reaction. Detailed measurements were made with N<sub>2</sub> gas targets; H<sub>2</sub> targets produced less scattering. We have somewhat arbitrarily increased the estimated uncertainty in the He<sup>++</sup>+H<sup>+</sup> cross section to +15% in all gases at our lowest energy. We demonstrated that no corrections were necessary at higher energies.

<sup>10</sup>J. B. Marion, *Rev. Mod. Phys.* **33**, 139 (1961).

<sup>11</sup>S. K. Allison and M. Garcia-Munoz, in *Atomic and Molecular Processes*, edited by D. R. Bates (Academic, New York, 1962), Chap. 19.

<sup>12</sup>L. I. Pivovarov, V. M. Tobaev, and M. T. Novikov, *Zh. Eksperim. i Teor. Fiz.* **41**, 26 (1961) [*Sov. Phys. JETP* **14**, 20 (1962)]; *Zh. Eksperim. i Teor. Fiz.* **42**, 1490 (1962) [*Sov. Phys. JETP* **15**, 1035 (1962)].

<sup>13</sup>V. S. Nikolaev, I. S. Dmitriev, L. N. Fateeva, and Ya. A. Teplova, *Zh. Eksperim. i Teor. Fiz.* **40**, 989 (1961) [*Sov. Phys. JETP* **13**, 695 (1961)].

<sup>14</sup>P. R. Jones, F. P. Ziembra, H. A. Moses, and E. Everhart, *Phys. Rev.* **113**, 182 (1959).

<sup>15</sup>H. B. Gilbody, J. B. Hasted, J. V. Ireland, A. R. Lee, E. W. Thomas, and A. S. Whiteman, *Proc. Roy. Soc. (London)* **A274**, 40 (1963).

<sup>16</sup>F. J. De Heer, J. Schutzen, and H. Moustafa, *Physica* **32**, 1793 (1966).

<sup>17</sup>A. B. Wittkower, G. Levy, and H. B. Gilbody, *Proc. Phys. Soc. (London)* **91**, 862 (1967).

<sup>18</sup>Pulse-height analysis of the mass-5 peak on the HeH<sup>+</sup> detector showed two slightly shifted energies, the main peak and a much smaller peak with approximately 5% higher energy deposited in the detector. We assume this second peak was due to D<sub>2</sub>H<sup>+</sup>, which apparently produced more charge in the detector than the <sup>3</sup>He in <sup>3</sup>HeD<sup>+</sup>. This assumption is strengthened by the fact that we also observed H<sup>+</sup> collision products.

<sup>19</sup>K. H. Berkner, T. J. Morgan, R. V. Pyle, and J. W. Stearns, Lawrence Radiation Laboratory Report No. UCRL-20821, 1971 (unpublished).